

Usage of Machine Learning for Subtopology Detection in Wire and Arc Additive Manufacturing

Dimitri Bratzel, Stefan Wittek, Andreas Rausch

Institute of Software and Systems Engineering
Technische Universität Clausthal
Clausthal-Zellerfeld, Germany
email: switt@tu-clausthal.de

Kai Treutler, Tobias Gehling, Volker Wesling

Institute of Welding and Machining
Technische Universität Clausthal
Clausthal-Zellerfeld, Germany
email: office@isaf.tu-clausthal.de

Abstract - In additive manufacturing, knowledge of the geometry of the weld seam is crucial for the quality of the component. This is especially true for Wire and Arc Additive Manufacturing (WAAM) based on Gas Metal Arc Welding (GMAW). The length of the free wire electrode ("stickout") should be almost constant during the entire manufacturing process. In additive manufacturing, it is also important to recognize height differences that occur during the process and to compensate for them by adjusting the process parameters in order to achieve a uniform build rate across the component cross-section, as geometric irregularities tend to be amplified by multiple layers. Furthermore, process disturbances can lead to locally altered seam properties. To counteract these problems, the presented investigations show to what extent such geometric irregularities can be detected in-situ from the existing process variables welding current and voltage. This makes it possible to dispense with the use of additional measurement technology. In our experiments, we simulated these height differences during multilayer welding by means of defined unevenness on the substrate plate. With the help of a Long Short Memory Neuronal Network (LSTM), the height information is determined indirectly during the process only via welding current and voltage. It is shown that this approach could be used to control the process. Furthermore, it is shown that this approach can reliably detect geometry errors and determine the height information with high accuracy, even if the process parameters are changed between training and validation.

Keywords: WAAM, Welding, GMAW, Machine Learning, Long Short-Term Memory, topology detection

I. INTRODUCTION

In order to ensure consistent weld seam quality, even in automated welding processes, with slightly changing geometric boundary conditions, a wide variety of sensor-based detection systems are currently being used. Among other things, the shape of the seam is detected by laser-based systems, usually using the light-sectioning method, to enable good seam tracking. On the other hand, the size of the melt pool is observed by optical systems [1]. An overview of the current state of research on monitoring and control of additive manufacturing is given in [2–4]. In addition to the dimension of the molten pool, conclusions can also be drawn here about the cooling of the weld seam or solidification. This not only allows the geometry of the weld to be determined, but also allows material properties to be specifically adjusted via the

cooling. Thus, the monitoring of the welding process represents a multi-criteria task, especially in the case of a weld-property orientation in additive manufacturing. One approach to solve such a multi-criteria task in advance has been shown by Ehlers et. al. in [5]. Due to increasingly complex applications of common welding processes, such as additive manufacturing, the task is also becoming more complex and sensory monitoring is becoming more important [6–9].

Complex, multi-criteria tasks can be solved using various artificial intelligence methods and, most importantly, can be computed in real time. Real-time computability is one of the main requirements for in-situ welding process monitoring and control, especially to be able to realize a material property oriented welding sequence as, e.g. in [5][10]. In these works, the cooling time between metallurgically important temperatures was used as a controlled variable, such as the $t_{8/5}$ -time concept to keep the material properties within a desired range.

In the following, a way to determine the geometry of the substrate for a weld bead based on welding current and voltage using artificial intelligence is presented. The aim is to derive further parameters from the existing process parameters without measuring them directly. This opens up the perspective of a material property- or geometry-oriented welding process control for metal inert gas welding.

The results presented in this paper were discussed in German language in [11].

A. Machine learning in welding and WAAM

The accurate prediction of the complex WAAM Process using numerical models is challenging and as of today, there exists no such model that could reliably predict the outcome of the process, outside very narrow experimental frameworks. Even if such a model would exist, the required computation time may easily make it impractical for the online monitoring tasks addressed in this paper. This is the reason why we focus on machine learned models, which can be trained, only using captured inline process data and can be inferred very fast, so that the online approach becomes viable. A number of other authors have committed works tackling this topic.

One major direction of the works lays in the prediction of some aspects of the overall outcome of the process based on parameters of the whole run. Most of these works rely on Artificial Neuronal Networks (ANN). One such approach

predicts the mean width and height of the weld based on the mean current and voltage using fixed feed and tool speeds [12]. Another approach relies on a set of process parameters including energy and feed speed, as well as tool speed [13]. In [14], this approach is even extended to not only predict the overall geometry but also the distortion that may occur. In [15], a hybrid approach is presented, using the ANN to predict the temperature distribution of the weld and then use this as an input for an FEM model to come to the stress and strain of the underlying metal sheet. Another parameter of the resulting weld that can be predicted this way is the surface roughness [16][17]. Common to all of these approaches is, that all of them use simple feed forward architectures to do regression from process parameters to outcome quantities. This has little in common with the idea of an inline approach where every measured value is directly used to predict some hidden value, such as the sub topology.

There are some works, mainly from the point of view of a control engineer, that forester such an inline view. In [18], for example, ANN are used to predict the temperature of a top layer based on the temperature of the layer underneath it. Other approaches are focused on online image recognition and the corresponding convolutional neuronal network architectures to interpret inline imagery. In [19], image recognition on IR cameras is used to preprocess the obtained images to then measure weld pool geometry using classical methods. Another example application for image recognition lays in detecting humps and valleys in the weld using a HDR camera sensing the process [20]. In [21], a very different approach is used. Here reinforcement learning is employed in order to control the geometry using inter layer scans of the top layer as an input.

While the results of this are promising, they require to bring new sensory into the process, which on the one hand, may be costly, and become an additional source of system failure. Additionally, none of the presented approaches treats the measured sensory data as a time series. This is due to the architectures for the neuronal networks chosen. This paper overcomes this shortage by using a network architecture suitable for this task. In the past, Long Short Term Memory neuronal networks (LSTM) have proven to be very suitable for predictions based on time series data [22].

While ANNs do stateless regression from a domain X to an image space Y, LSTM are able to internally keep a state based on the last observer sensory values X and perform a prediction of Y based on these past observations. In section II the used materials and methods for the welding experiments

carried out and the used neuronal network will be described. Followed by Section III presenting the results and Section IV in which the results are discussed.

II. MATERIALS AND METHODS

To record the training and comparison data for the neural networks used, a "Fronius TransPuls Synergic 4000 CMT" welding power source was coupled with a robot from Kuka as an automated motion system and equipped with a laser triangulation displacement sensor type optoNCDT 1420 from MICRO-EPSILON for distance measurement. The current and voltage signals, as well as the distance measurement values were recorded with a "Scope Corder DL750" from Yokogawa. To create defined height differences in the substrate, the substrate plate was provided with elevations and grooves, Figure 1.

The grooves are 4 mm deep and the elevations 4 mm high. The grooves and elevations have an angle of 90°. These selected defined changes are in the upper range of typical seam irregularities and seam defects. Depending on the choice of process adjustment variables, an GMA-weld can have a height of 1mm to 9mm and a width between 2.5mm and 20mm.

A total of ten welding tests were carried out. Welding was carried out across the tests as follows:

Welding consumable:	ISO14341-A-G 4Mo
Wire electrode diameter:	1.2 mm
Shielding gas:	82% Ar / 18% CO ₂
Welding speed:	55 cm/min
Stick-out:	15 mm
Base material:	S355

The wire feeds, the resulting average current and voltage values and the set process can be taken from Table 1. In addition to different wire feeds, both the standard and the impulse welding process were used.

The experimental setup is sketched in Figure 2.a, with the welding direction out of the image plane. To measure the changes in distance between the displacement sensor and the substrate material, the arc of light was shielded from the sensor. Figure 2b shows a sketch of the substrate plate used.



Figure 1: Side view of the base plate

TABLE 1: EXPERIMENTAL CONDITIONS

Run. Nr.	Wire feed speed	Current	Voltage	Welding Mode
1	4,5	93	17,0	Impulse
2	4,5	93	17,0	Impulse
3	4,5	93	17,1	Impulse
4	4,8	136	14,5	Standard
5	4,8	136	14,5	Standard
6	4,8	136	14,6	Standard
7	7,0	171	16,2	Standard
8	1,7	37	14,7	Impulse
9	1,7	37	14,2	Impulse
10	1,7	37	15,2	Impulse

A. Methodology in the use of artificial intelligence

The collected raw data of the 10 tests consist of the measured quantities: voltage [volts], current [amps] and distance [mm]. The measurement data of tests 3, 9 and 10 had to be discarded due to recording errors. Voltage and current are the input variables, with the help of which height differences should be indirectly predicted. To eliminate extreme outliers, a filter was applied. For the distance, values larger than 190 mm and smaller than 160 mm were removed. For voltage, values greater than 40 V and less than 10 V were eliminated. Furthermore, the distance measurement exhibits noise that occurs at regular intervals, with an amplitude of about +/-4 mm and a period of oscillation of a few milliseconds. Since the defined geometry irregularities are in a comparable order of magnitude, it is necessary to clean this noise to obtain good labels for training the LSTM. Furthermore, the input quantities have voltage and current typical characteristics with very high amplitudes and extreme values, which were identified as measurement errors. All three quantities were preprocessed in two steps. In the first step, the moving average method was used with a triangular weighting and a window width of 10,000 measurement points. In the

second step, averaging was applied, reducing the total number of measurement points from about 3 million per experiment to about 900 to 1,000 measurement points. This eliminated most of the periodic oscillations and outliers. Figure 3 shows all three measured variables. For the illustration, the values were scaled in preparation for the training. By reducing the number of measurement points, the scaling of the x-axis (previously time) is lost. Only the sequence of data points is shown. It can be seen that there is a correlation between the input variables (current and voltage) and the output variable (distance).

For each experiment, a model with the same network architecture was trained. As a result, seven models were available, each of which was trained on one experiment.

The input values are stored as a three-dimensional tensor, whereby a label with a corresponding distance measurement is available for a series of data. During the learning process, the neural network looks at the past 50 values (the time window chosen in this analysis) and deduces the current distance from the torch to the workpiece. Since the input is a sequence of current and voltage values and only one distance value is to be predicted, a funnel-shaped architecture of the LSTM was chosen. The models were implemented in Python

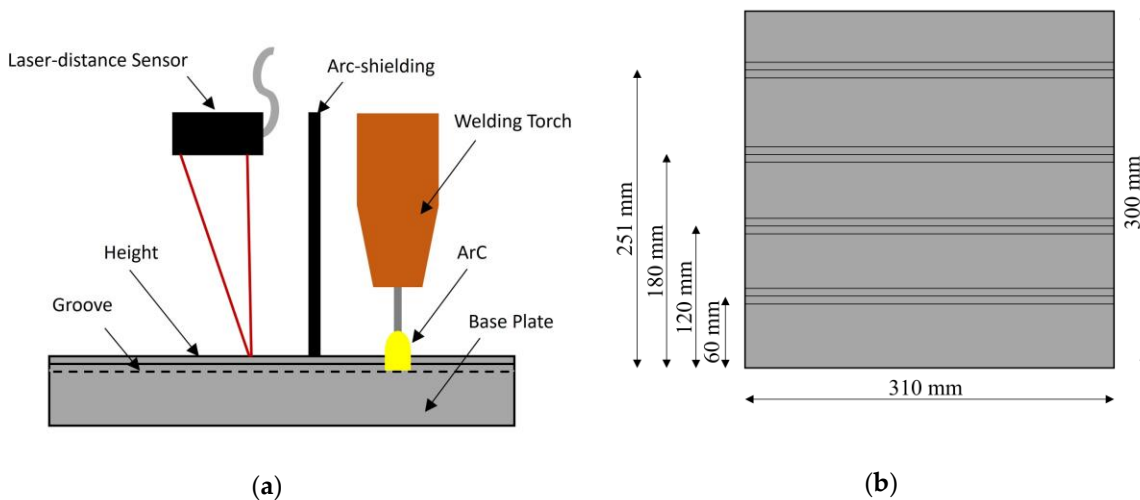


Figure 2: principle sketch of the experiment: a) experimental setup, b) substrate plate

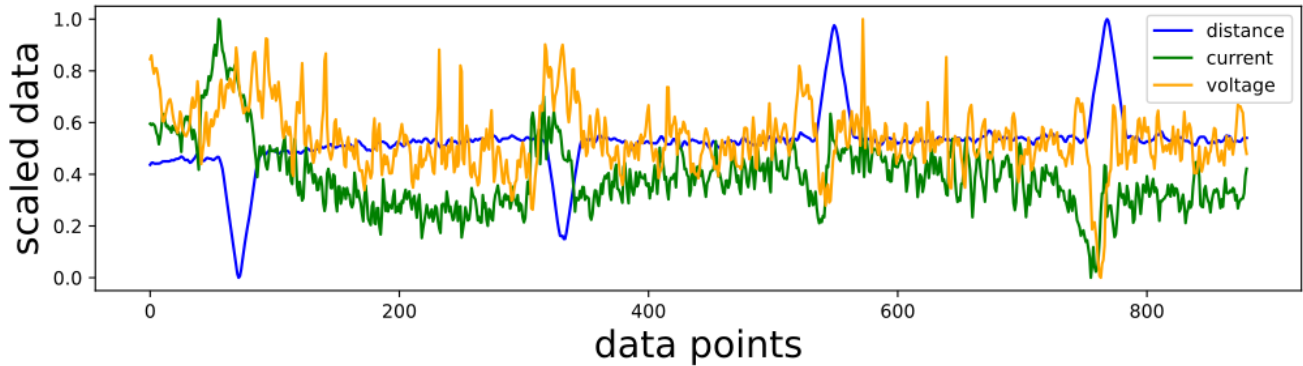


Figure 3: Scaled and preprocessed measured values of experiment 1

using the KERAS framework. The corresponding parameterization of the network with two layers and neurons: Layer₁ = 50 and Layer₂ = 20. There is only one neuron in the output layer, this one carries the value of the distance. The "Mean Squared Error" serves as the "loss function" or cost function and "ADAM" was chosen as the method of stochastic optimization. Only for experiment 7 a bias regulator (L2=0,1) was used additionally, because the model showed typical signs of overfitting. All models were trained over 500 epochs, with a batch size of 60.

III. RESULTS

Within the experiments, the first two thirds were used as training data. On the last third, the model was tested (see Figure 4). In addition, the generalization of the models

between the experiments was tested. This was only successful between trials with the same procedure (impulse or standard). In each case, the models were applied to an entirely different data set. Figure 5 shows the Mean Absolute Deviation (MAE) of the models (rows) when applied to the different tests (columns) for the tests with impulse (a) and standard (b) methods. This can be interpreted as the mean deviation of the predicted profile from the actual profile. The maximum deviation is 0.29 mm, the minimum 0.18 mm.

The models perform differently if used to predict profiles of experiments not used for training. The mean absolute error form most cases (except for experiment 8), remains well below one millimeter, even in this cross-experiment setup.

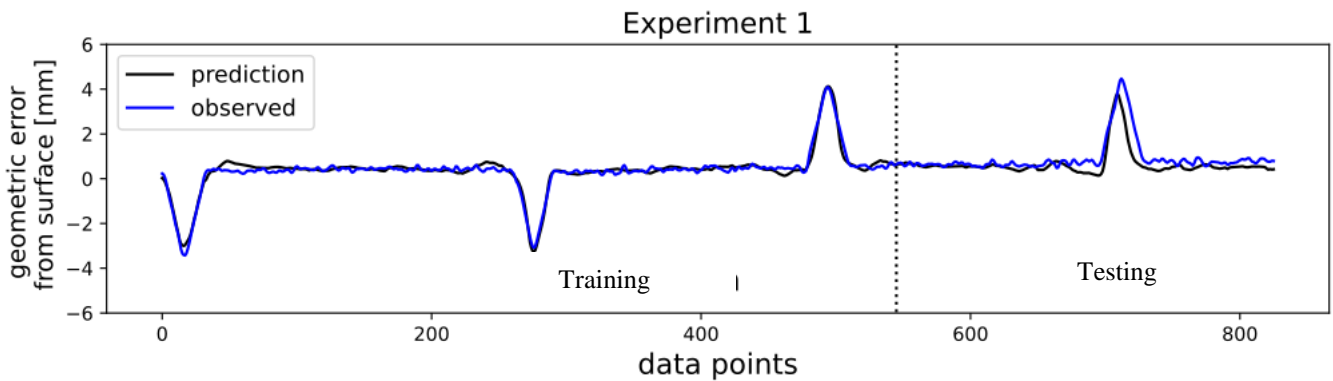


Figure 4: Prediction accuracy in the training and test area, experiment 1

	impulse process MAE			standart process MAE				
	experiment_1	experiment_2	experiment_8	experiment_4	experiment_5	experiment_6	experiment_7	
a) model_1	0,29 mm	0,43 mm	0,66 mm	model_4	0,25 mm	0,3 mm	0,39 mm	0,48 mm
model_2	0,35 mm	0,18 mm	0,63 mm	model_5	0,27 mm	0,22 mm	0,3 mm	0,68 mm
model_8	2,1 mm	1,7 mm	0,21 mm	model_6	0,29 mm	0,31 mm	0,25 mm	0,39 mm
b) model_7				model_7	0,36 mm	0,37 mm	0,46 mm	0,25 mm

Figure 5: Mean Absolute Deviation of all tests

IV. DISCUSSION

In the presented work, it was shown that the use of neural networks allows to estimate the substrate topography in GMA-welding with high accuracy. Furthermore, it was shown that even with a small number of training experiments and a limited database for different process variants, small deviations of the prediction from the actual value in the lower tenth of a millimeter range could be achieved. The work presented is promising. Therefore, they are to be extended to real welding tests and to the application in additive manufacturing using larger data bases and further process parameters such as the light emitted by the arc, as well as the melt pool size and the temperature distribution. Although the chosen LSTM network architecture proved to be capable for the application described, additional comparative experiments using a wide array of methods is needed.

V. CONCLUSION

The work conducted in this paper shows that the usage of a neuronal network for the prediction of the stick-out and/or the geometry of the topologies beneath the actual weld seam is possible. It was possible to generate the necessary database for teaching the network in only a few experiments. Even this relatively low number of experiments resulted in a prediction accuracy that is sufficiently precise for the application. As mentioned above one obvious direction for further work lays in transferring the approach from a single layer welding experiment to actual additive manufacturing in multiple layers. Another direction is to close the loop by implementing a controller based on the predicted subtopology to compensate errors. This is by no means trivial, since the control algorithm itself would interfere with voltage and current, thusly challenging the prediction capability of the network.

REFERENCES

- [1] A. Richter, T. Gehling, K. Treutler, V. Wesling, and C. Rembe, "Real-time measurement of temperature and volume of the weld pool in wire-arc additive manufacturing," *Measurement: Sensors* 2021, 17, pp. 100060-100069, doi:10.1016/j.measen.2021.100060.
- [2] K. Treutler and V. Wesling, "The Current State of Research of Wire Arc Additive Manufacturing (WAAM): A Review," *Applied Sciences* 2021, 11, pp. 8619-8625, doi:10.3390/app11188619.
- [3] S. Singh, S. K. Sharma, and D. W. Rathod, "A review on process planning strategies and challenges of WAAM," *Materials Today: Proceedings* 2021, 47, pp. 6564-6575, doi:10.1016/j.matpr.2021.02.632.
- [4] C. Xia, et al., "A review on wire arc additive manufacturing: Monitoring, control and a framework of automated system," *Journal of Manufacturing Systems* 2020, 57, pp. 31-45, doi:10.1016/j.jmsy.2020.08.008.
- [5] R. Ehlers, K. Treutler, and V. Wesling, "SAT Solving with Fragmented Hamiltonian Path Constraints for Wire Arc Additive Manufacturing," In *Theory and Applications of Satisfiability Testing - SAT 2020*; Pulina, Hofmann, Eds.; Springer International Publishing: [S.l.], 2020; pp. 492-500, ISBN 978-3-030-51824-0.
- [6] A. Chabot, M. Rauch, and J.-Y. Hascoët, "Towards a multi-sensor monitoring methodology for AM metallic processes," *Weld World* 2019, 63, pp. 759-769, doi:10.1007/s40194-019-00705-4.
- [7] C. Halisch, T. Radel, D. Tyralla, and T. Seefeld, "Measuring the melt pool size in a wire arc additive manufacturing process using a high dynamic range two-colored pyrometric camera," *Weld World* 2020, 64, pp. 1349-1356, doi:10.1007/s40194-020-00892-5.
- [8] X. Wang, A. Wang, and Y. Li. „An online surface height measurement method for GTAW-based additive manufacturing," *Weld World* 2020, 64, pp. 11-20, doi:10.1007/s40194-019-00813-1.
- [9] A. Waqas, X. Qin, J. Xiong, H. Wang, and C. Zheng, „Optimization of Process Parameters to Improve the Effective Area of Deposition in GMAW-Based Additive Manufacturing and its Mechanical and Microstructural Analysis," *Metals* 2019, 9, pp. 775-798, doi:10.3390/met9070775.
- [10] K. Treutler, S. Kamper, M. Leicher, T. Bick, and V. Wesling. "Multi-Material Design in Welding Arc Additive Manufacturing," *Metals* 2019, 9, pp. 809-823, doi:10.3390/met9070809.
- [11] D. Bratzel, S. Wittek, A. Rausch, K. Treutler, T. Gehling, and V. Wesling. „Using AI Methods for Subtopology Detection in MSG-Welding“ i.o. „Nutzung von KI-Methoden zur Geometriedetektion beim MSG-Schweißen," In *Tagungsband 4. Symposium Materialtechnik*; Clausthaler Zentrum für Materialtechnik, Ed.; Shaker Verlag: Düren, 2021; pp. 127–136, ISBN 978-3-8440-8021-6.
- [12] G. O. Barrionuevo, S. Rios, S. W. Williams, and J. Andres Ramos-Grez, "Comparative Evaluation of Machine Learning Regressors for the Layer Geometry Prediction in Wire arc Additive manufacturing," In *2021 IEEE 12th International Conference on Mechanical and Intelligent Manufacturing Technologies (ICMIMT)*; IEEE, 2021; pp. 186-190.
- [13] J. Deng, Y. Xu, Z. Zuo, Z. Hou, and S. Chen, "Bead Geometry Prediction for Multi-layer and Multi-bead Wire and Arc Additive Manufacturing Based on XGBoost,"

- Transactions on Intelligent Welding Manufacturing*; Springer, Singapore, 2019; pp. 125-135.
- [14] C. Wacker, et al. , “Geometry and Distortion Prediction of Multiple Layers for Wire Arc Additive Manufacturing with Artificial Neural Networks,” *Applied Sciences* 2021, *11*, pp. 4694-4709 , doi:10.3390/app11104694.
- [15] Q. Wu, T. Mukherjee, A. De, and T. DebRoy, “Residual stresses in wire-arc additive manufacturing – Hierarchy of influential variables,” *Additive Manufacturing* 2020, *35*, pp. 101355-101327, doi:10.1016/j.addma.2020.101355.
- [16] C. Xia, et al., “Modelling and prediction of surface roughness in wire arc additive manufacturing using machine learning,” *J Intell Manuf* 2021, pp. 1-16, doi:10.1007/s10845-020-01725-4.
- [17] A. Yaseer and H. Chen, “Machine learning based layer roughness modeling in robotic additive manufacturing,” *Journal of Manufacturing Processes* 2021, *70*, pp. 543-552, doi:10.1016/j.jmapro.2021.08.056.
- [18] P. K. Nalajam and R. Varadarajan, “A Hybrid Deep Learning Model for Layer-Wise Melt Pool Temperature Forecasting in Wire-Arc Additive Manufacturing Process,” *IEEE Access* 2021, *9*, pp. 100652-100664, doi:10.1109/access.2021.30971177.
- [19] Y. Wang, et al., “Active disturbance rejection control of layer width in wire arc additive manufacturing based on deep learning,” *Journal of Manufacturing Processes* 2021, *67*, pp. 364-375, doi:10.1016/j.jmapro.2021.05.005.
- [20] C. Lee, G. Seo, D. B. Kim, M. Kim, and J.-H. Shin, “Development of Defect Detection AI Model for Wire + Arc Additive Manufacturing Using High Dynamic Range Images,” *Applied Sciences* 2021, *11*, pp. 7541-7560, doi:10.3390/app11167541.
- [21] A. G. Dharmawan, Y. Xiong, S. Foong, and G. Song Soh. “A Model-Based Reinforcement Learning and Correction Framework for Process Control of Robotic Wire Arc Additive Manufacturing,” In *2020 IEEE International Conference on Robotics and Automation (ICRA)*; IEEE, 2020; pp. 4030-4036.
- [22] F. A. Gers, J. Schmidhuber, and F. Cummins. “Learning to forget: continual prediction with LSTM,” *Neural Computation* 2000, *12*, pp. 2451-2471, doi:10.1162/089976600300015015.